Search for a gravitational wave background from primordial black hole binaries using data from the first three LIGO-Virgo-KAGRA observing runs

Tore Boybeyi,[1,*] Sebastien Clesse,[2,3,†] Sachiko Kuroyanagi,[4,5,‡] and Mairi Sakellariadou[6,§]

[1]*School of Physics and Astronomy, University of Minnesota, Minneapolis, Minnesota 55455, USA*
[2]*Service de Physique Théorique Brussels Laboratory of the Universe, Université Libre de Bruxelles, Boulevard du Triomphe, CP225, 1050 Brussels, Belgium*
[3]*Brussels Laboratory of the Universe, Université Libre de Bruxelles, Boulevard du Triomphe, CP225, 1050 Brussels, Belgium*
[4]*Instituto de Física Teórica UAM-CSIC, Universidad Autónoma de Madrid, Cantoblanco 28049 Madrid, Spain*
[5]*Department of Physics and Astrophysics, Nagoya University, 464-8602, Nagoya, Japan*
[6]*Theoretical Particle Physics and Cosmology Group, Physics Department, King's College London, University of London, Strand, London, WC2R 2LS, United Kingdom*

(Received 2 January 2025; accepted 13 June 2025; published 28 July 2025)

Using the cross-correlation data from the first three observing runs of the LIGO-Virgo-KAGRA collaboration, we search for a gravitational-wave background (GWB) from primordial black holes, arising from the superposition of compact binary coalescence events. We consider both early and late binary formation mechanisms and perform Bayesian parameter inference. From the nondetection of the GWB, we provide constraints on the fraction of primordial black holes contributing to the present dark matter energy density.

DOI: 10.1103/zphk-3ld9

I. INTRODUCTION

Gravitational-wave (GW) astronomy has the potential to revolutionize our understanding of the Universe by providing insights into its most energetic and dynamic phenomena. GW detections allow us to explore regions of space-time that are inaccessible through electromagnetic observations. Since the first binary black hole (BBH) merger detected by the LIGO-Virgo-KAGRA (LVK) collaboration [1], the field has rapidly expanded with numerous GW events reported over the past decade [2–4]. These observations have advanced our knowledge of compact objects, their merger mechanisms, and have enabled tests of general relativity in the strong-field regime [5]. Additionally, GW signals have been used to measure the Hubble constant through standard sirens [6].

Beyond individual events, the gravitational wave background (GWB)—a collective signal from many *unresolved* sources—provides a powerful tool for probing both astrophysical and cosmological processes. Astrophysical contributions to the GWB arise from unresolved BBH, binary neutron star, and black hole–neutron star mergers throughout cosmic history [7]. These compact binaries may form via various channels, including isolated binary evolution and dynamical interactions in dense stellar environments. On the cosmological side, potential GWB sources include phase transitions in the early universe [8,9], cosmic strings [10,11], and primordial fluctuations from inflation [12]. Detecting a cosmological GWB would open a new window into the physics of the early universe and high-energy phenomena beyond the reach of particle accelerators [13,14].

In this article, we focus on primordial black holes (PBHs), which are hypothesized to form from the collapse of large density fluctuations in the early universe [15]. Unlike astrophysical black holes, which are remnants of massive stars, PBHs can span a wide range of masses, from asteroidlike to supermassive scales, depending on the model. PBHs are gaining particular attention as they offer unique insights into conditions in the early universe, such as the spectrum of primordial density fluctuations, phase transitions, and inflationary physics. Moreover, PBHs are considered potential candidates for dark matter [15–18] and for observed compact binary coalescences (CBCs) [19–21].

Several previous studies have investigated the possibility that some of the detected CBC events originate from PBH mergers [22–42]. These studies typically analyze the

*Contact author: boybe001@umn.edu
†Contact author: sebastien.clesse@ulb.be
‡Contact author: sachiko.kuroyanagi@csic.es
§Contact author: mairi.sakellariadou@kcl.ac.uk

Published by the American Physical Society under the terms of the Creative Commons Attribution 4.0 International license. Further distribution of this work must maintain attribution to the author(s) and the published article's title, journal citation, and DOI.

observed population of CBCs obtained through individual detections by examining their mass distributions, spin orientations, and redshift distributions to discuss whether the properties of these events are consistent with an astrophysical origin or suggest a primordial origin. For example, a BBH merger with component masses in the so-called "mass gap" region—where standard stellar evolution models predict a scarcity of black holes due to pair-instability supernovae—has prompted speculation about a primordial origin [30,31,38,43,44]. Furthermore, a subsolar mass event can serve as distinct evidence of PBHs [45–48].

These analyses compare the observed GW event rates with the predicted merger rates from PBH populations. Note, however, that LVK binary abundance constraints rely on calculations showing that PBHs form binaries very efficiently in the early universe, treating PBHs as constant Schwarzschild masses. This assumption is not well justified, since during such early times the Hubble horizon is still small. Consequently, one cannot ignore the fact that these PBHs are embedded in an expanding background [49].

Another approach is to search unresolvable binaries as a GWB. Some studies have explored constraints on PBHs by considering the GWB produced by their mergers, a line of research pioneered in [50]. Constraints have been discussed in the literature [25,27,51–55], typically involving a rough comparison between theoretical predictions and the upper bounds obtained from the isotropic GWB search performed by the LVK collaboration [56–58], which assumes a power-law spectrum $\Omega_{\rm GW} \propto f^{\alpha}$. Although this assumption may be valid for a GWB originating from an unresolved BBH population from population I or II stars (where lower end is bounded by the Chandrasekhar limit, while the intermediate mass range is constrained by pair instability), PBH mass distributions can extend significantly beyond $\sim 50 M_{\odot}$. As a result, the GWB spectrum could deviate from a simple power-law form when PBH sources are considered ([55]).

Motivated by these, we analyze public GWB data from the first three LVK observing runs (O1–O3) [56–58] and perform a full Bayesian parameter inference for the GWB from PBHs with a wide range of masses, including subsolar masses up to 10^3 solar masses. This allows us to account for the complete spectral shape and explore a broad parameter space that extends beyond the detection of individual mergers by LVK. Some recent works in this direction are [42,55], although the former was primarily focused on distinguishing between astrophysical and primordial BBHs. In addition, the PBH model used in [42,55] was limited to a single mass bin of 1 and $30 M_{\odot}$. It is worth noting that in what follows it is for the first time considered the combination of different formation channels to get corresponding constraints and assess their relative significance.

In what follows, we aim to effectively bridge the gap between theoretical studies and observational data through robust Bayesian analysis. Updating to the most up-to-date publicly available data from the LVK (O1–O3) searches, we provide more reliable and comprehensive constraints on PBH abundance for peaked mass distributions across a broad mass range, a topic gaining significant attention in the field, particularly in relation to other cosmological constraints. The Bayesian framework offers key advantages in this context. It is a natural framework to include various constraints between parameters and uncertainties on them into the analysis. Moreover, in the event of a future GWB detection, Bayesian inference will be essential for identifying the underlying source population and distinguishing between astrophysical and primordial origins.

The paper is organized as follows. In Sec. II, we describe the models for calculation of the PBH merger rate. In Sec. III, we outline our Bayesian inference method and present the results. Then we conclude in Sec. IV. Appendix A provides additional details on the suppression factors relevant to the early binary formation scenario. Appendix B describes the cross-correlation statistics used in our analysis. Appendix C presents an injection study exploring various potential scenarios. Appendix D provides the posterior distributions of all parameters corresponding to the main results.

II. MODELING

To parametrize the abundance of PBH, we commonly use $f_{\rm PBH} = \Omega_{\rm PBH}/\Omega_{\rm DM}$, which is the fraction of PBH in the dark-matter energy density today. One of the key factors influencing the GW spectrum in our model is the mass function of PBHs. It is commonly parametrized using monochromatic or log-normal distributions. They may not accommodate a mass function with a detailed shape, such as the one associated with the QCD phase transition [59–61], but it is a good approximation for PBHs arising from a peak in the primordial power spectrum [62].

Using the PBH energy density $\rho_{\rm PBH}$, we define the PBH mass function $p(m)$ as

$$p(m) = \frac{1}{\rho_{\rm PBH}} \frac{{\rm d}\rho_{\rm PBH}}{{\rm d}\ \ln\ m}. \tag{1}$$

For a log-normal Gaussian distribution of the PBH mass function, we have

$$p(m) = \frac{1}{\sqrt{2\pi}\sigma} \exp\left[-\frac{(\ln\ m - \ln\ \mu)^2}{2\sigma^2}\right]. \tag{2}$$

The mass function is normalized to satisfy $\int p(m) {\rm d} \ln m = 1$ and is usually motivated by inflationary scenarios [63]. We concentrate on relatively narrow mass distributions ($\sigma < 1$) because theoretical predictions for broader distributions contain significant uncertainties [62,64–66]. Nevertheless, our chosen distribution remains sufficiently broad within the LVK sensitivity range, allowing mass variations on the order of the central value [$\sim \mathcal{O}(\mu)$], potentially spanning several tens of solar masses around $\sim 50 M_{\odot}$. While our

simple log-normal distribution represents progress towards understanding these mass distributions, detailed modeling incorporating more complex structure will be deferred to future work.

The amplitude of the GWB is often characterized by the dimensionless parameter

$$\Omega_{\rm GW} \equiv \frac{1}{\rho_{c,0}} \frac{{\rm d}\rho_{\rm GW}}{{\rm d}\ \ln\ f}, \tag{3}$$

where $\rho_{c,0} = 3H_0^2/(8\pi G)$ is the critical density of the Universe today. The GWB formed by the ensemble of CBC events can be calculated by summing up the energy spectrum of each binary system, divided by $(1+z)$ to account for the redshifting of the gravitons since emission and taking into account the merger rate distribution [67],

$$\Omega_{\rm GW}(f) = \frac{f}{\rho_{c,0}} \int_0^{z_{\rm max}} {\rm d}z \int {\rm d}\ \ln\ m_1\, {\rm d}\ \ln\ m_2 \frac{p(m_1)p(m_2)}{(1+z)H(z)} \times \frac{d^2R_{\rm EB/LB}}{d\ \ln\ m_1 d\ \ln\ m_2} \frac{{\rm d}E_{\rm GW}}{{\rm d}f_{\rm r}}, \tag{4}$$

where $f_{\rm r} = (1+z)f$ is the GW frequency in the source frame. Here $\frac{d^2R_{\rm EB/LB}}{d\ \ln\ m_1\, d\ \ln\ m_2}$ describes the differential merger rate per unit time, comoving volume, and mass interval where EB and LB stand for "early binary" and "late binary," respectively, and denote different binary formation mechanisms described in the next subsection. ${\rm d}\,E_{\rm GW}/{\rm d}f_r$ is the single source energy spectrum, which is a function of the masses of the compact objects, m_1 and m_2; its fitting function including inspiral, ringdown, and merger phases is given in [68].

A. Early binary formation

Early binaries are formed in the radiation-dominated era shortly after PBH formation. In this scenario, a binary is formed from a pair of closely spaced PBHs with the surrounding third object acting on the pair via a tidal force that generates the angular momentum of the binary [20,69]. The merging rate (per unit logarithmic mass of the two binary components) of early binaries at a time t is given by [20,23,26,70,71]

$$\frac{d^2R_{\rm EB}}{d\ln m_1\, d\ln m_2} = \frac{1.6\times10^6}{{\rm Gpc}^3\ {\rm yr}} f_{\rm PBH}^{53/37} \left[\frac{t}{t_0}\right]^{-34/37} \times \left(\frac{m_1+m_2}{M_\odot}\right)^{-32/37} \left[\frac{m_1 m_2}{(m_1+m_2)^2}\right]^{-34/37} \times S(m_1, m_2, f_{\rm PBH}), \tag{5}$$

where m_1 and m_2 are the two black hole masses and t_0 is the age of the Universe. A rate suppression factor, S, has been introduced to account for two principal mechanisms that impede binary formation due to local matter inhomogeneities and nearby PBHs $S_1(m_1, m_2, f_{\rm PBH})$ and the clustering due to their initial Poissonian fluctuations $S_2(f_{\rm PBH})$ [26,27]. Analytical prescriptions for these suppression factors have been studied in [26,27] which are shown to be consistent with numerical simulations [26]. We detail these aspects in Appendix A, including the relevant ranges for our work and their limitations.

B. Late binary formation

Late binaries form much later due to dynamical capture in the clusters of PBHs during the matter-dominated era [19]. For a general mass distribution of PBHs, an expression for the merger rate has been proposed in the literature [72,73]:

$$\frac{d^2R_{\rm LB}}{d\ln m_1 d\ln m_2} = \frac{R_{\rm clust}}{{\rm Gpc}^3\ {\rm yr}} f_{\rm PBH}^2 \frac{(m_1+m_2)^{10/7}}{(m_1 m_2)^{5/7}}. \tag{6}$$

$R_{\rm clust}$ is a single parameter that encapsulates how much the local environment of PBHs boosts their merger rate which depends on the velocity dispersion and density contrast in PBH. In the ΛCDM model without significant small-scale Poisson fluctuations, one typically finds low values in the range of a $O(1\sim10)$ [74] by applying the Press-Schechter formalism to the linear matter power spectrum. However, if PBHs make up most of the dark matter at around solar masses or above, their discrete (Poisson-like) distribution can seed dense subhalos that raise this factor into the $O(10^2$–$10^3)$ [30,75]. Current GW data from individually detected binaries, particularly from mergers near the neutron-star and pair-instability mass gaps, is consistent with $\sim 4\times10^2$ [30]. This value remains somewhat model dependent, since processes like direct cluster formation or varying PBH mass fractions can push it higher or lower, but the data suggest that a few hundred is a reasonable benchmark. To encapsulate these different cases, we will take three reference values for $R_{\rm clust} = [1, 4\times10^2, 10^3]$.

III. BAYESIAN SEARCH

A. Methodology

Let us outline the Bayesian framework employed in our search for GWB originating from PBHs and other compact binary sources. Our methodology was first introduced in [76] and closely follows that of previous studies [57,58,77–85], with specific adaptations to our analysis.

We utilize data from the Advanced LIGO detectors located in Hanford (H) and Livingston (L), as well as data from the Virgo (V) observatory, during the first three observing runs (O1–O3) [86–89]. Our search incorporates all available baselines (HL, HV, LV) (only HL baseline is available for O1 and O2) to maximize sensitivity and leverage the complementary geographical locations of the detectors.

Following the notation of [81], the primary observable is the cross-correlation estimator $\hat{C}_{IJ,f_i}$ which measures the correlation between detectors I and J as a function of discrete frequency f_i. This estimator is constructed by cross-correlating the discrete Fourier transforms of the outputs from different detectors. It is then transformed into the estimator $\hat{\Omega}^{IJ}_{\mathrm{GW},f_i}$ by multiplying with the relevant numerical factors and the overlap reduction function. These definitions are given in Appendix B. The likelihood function for the search of an isotropic GWB is [76,81]

$$p(\hat{\Omega}^{IJ}_{\mathrm{GW},f_i}|\boldsymbol{\theta},\lambda) \propto \exp\left[-\frac{1}{2}\sum_{IJ}\sum_{f_i}\left(\frac{\hat{\Omega}^{IJ}_{\mathrm{GW},f_i}-\lambda\Omega_{\mathrm{GW}}(f_i|\boldsymbol{\theta})}{\sigma^{IJ}_{f_i}}\right)^2\right], \tag{7}$$

where $\sigma^{IJ}_{f_i}$ denotes the variance of the cross-correlation estimator, which is derived from the noise power spectral density of each detector and $\Omega_{\mathrm{GW}}(f_i|\boldsymbol{\theta})$ represents the theoretical model to be compared with the data, characterized by a set of parameters $\boldsymbol{\theta}$. The sum runs over the frequency bins f_i as well as different pairs of the detectors labeled by $I, J = \mathrm{H}, \mathrm{L}, \mathrm{V}$. We then construct the posterior distribution using Bayes' theorem,

$$p(\boldsymbol{\theta},\lambda|\hat{\Omega}^{IJ}_{\mathrm{GW},f_i}) = \frac{p(\hat{\Omega}^{IJ}_{\mathrm{GW},f_i}|\boldsymbol{\theta},\lambda)p(\theta,\lambda)}{p(\hat{\Omega}^{IJ}_{\mathrm{GW},f_i})}. \tag{8}$$

We then marginalize over the calibration uncertainty parameter λ, as detailed in calibration uncertainty studies [81,90,91], to get $p(\boldsymbol{\theta}|\hat{\Omega}^{IJ}_{\mathrm{GW},f_i}) = \int d\lambda p(\lambda) p(\boldsymbol{\theta},\lambda|\hat{\Omega}^{IJ}_{\mathrm{GW},f_i})$.

B. Prior distributions

We employ a set of priors including the following parameters: the mean of the log-normal mass distribution μ, its width σ, and the PBH fraction f_{PBH} in the dark matter energy density today, as introduced previously.

We also take into account an additional otherwise individually unresolvable CBC background from astrophysical black holes which can include lighter binaries like neutron stars as well. Their spectrum is well approximated by a simple fiducial power law characterized by a single parameter, and is expressed as Ω_{cbc} as $\Omega_{\mathrm{CBC}}(f) = \Omega_{\mathrm{cbc}}(f/f_{\mathrm{ref}})^{2/3}$, with $f_{\mathrm{ref}} = 25$ Hz [56–58,92]. Deviations from this fiducial power law are not prominent and the expected CBC spectrum only deviates from the power law beyond the current sensitivity (e.g., Fig. 5 in [58]). Therefore, our model is $\Omega_{\mathrm{GW}} = \Omega_{\mathrm{CBC}} + \Omega_{\mathrm{EB}} + \Omega_{\mathrm{LB}}$.

The prior distributions for the model parameters are specified in Table I. These ranges encompass plausible values based on theoretical models and existing constraints [25,27,30,34,37,41,44,58,75]. We adopt a log-uniform prior for the PBH abundance f_{PBH} because a Jeffreys (log-uniform) prior is the least informative choice for a scale parameter—it assigns equal weight to each decade avoiding biasing the inference toward any particular order of magnitude [93]. We set the lower bound on f_{PBH} prior to 10^{-5} which is usually the standard choice [44,94]; this makes our results directly comparable to the existing literature.

TABLE I. Prior distributions for the model parameters in the Bayesian analysis. $\mathcal{LU}$ denotes a log-uniform distribution.

Parameter	Prior
Ω_{CBC}	$\mathcal{LU}(10^{-10}, 10^{-7})$
$\mu(M_\odot)$	$\mathcal{LU}(10^{-1}, 10^{3})$
σ	$\mathcal{LU}(10^{-2}, 10^{0})$
f_{PBH}	$\mathcal{LU}(10^{-5}, 1)$

C. Result

In order to perform Bayesian parameter inference, we employ the nested sampling algorithm from the Dynesty package [95] for robust parameter space exploration. To expedite the computation of integrals in the GW spectrum calculations, we utilize Sobol Monte Carlo integration [96], a quasirandom low-discrepancy sequence method that improves convergence rates over traditional Monte Carlo approaches, thereby reducing computational overhead. To account for calibration uncertainties in GW detector data, we use the Python library PYGWB [81], which integrates these uncertainties into the parameter estimation process.

Our analysis is based on the combined cross-correlation dataset from the first three observing runs of the LVK collaboration. We applied data quality cuts and vetoes following the procedures outlined in previous isotropic GWB searches by the LVK [56–58]. For parameter sampling, we utilized 5×10^4 live points with a convergence criterion of $d\ln(z) < 0.1$.

The results indicate that no significant GWB associated with PBHs or CBCs has been detected over the noise hypothesis, with logarithmic Bayes factors ~ -1 and corner plots in Figs. 4–6. We establish upper limits on the CBC energy density parameter, Ω_{cbc}, of $\sim 3 \times 10^{-9}$ at the 95% CL level which are consistent with LVK constraints [58].

From the nondetection, we can constrain the fraction of PBHs, f_{PBH}, as a function of the mean mass μ. The obtained constraint, along with other studies from lensing surveys like EROS [97], OGLE [98], supernova Ia [99], and cosmic microwave background (CMB) constraints for different R_{clust} choices are summarized in Fig. 1 and Table II. We also provide the resulting corner plots for all model parameters in Appendix D.

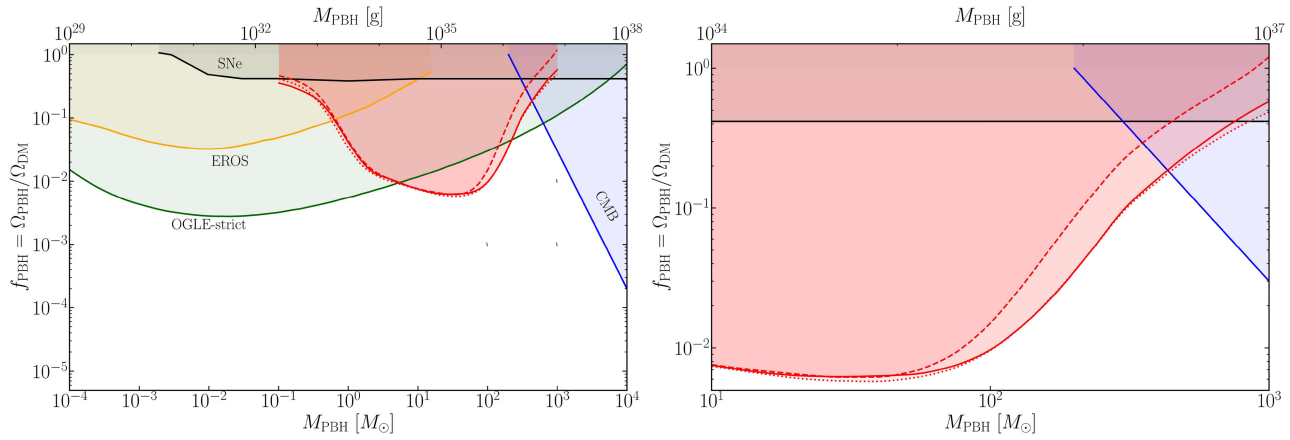


FIG. 1. Left: 95% CL constraints on $f_{\rm PBH}$ as a function of $M_{\rm PBH}(=\mu)$ from the search for the GWB using the different $R_{\rm clust}$ choices are shown in red (1 dashed, 4×10^2 solid, 10^3 dotted). We also display supernova lensing constraints (SNe) [99] in purple, massive compact halo object (MACHO) constraints [97] in orange designated as (EROS), the recent optical gravitational lensing experiment (OGLE) constraints are shown in green with different Milky Way models [98], and cosmic microwave background (CMB) constraints from [100]. We used the PBHBounds [101] to generate this plot. Right: enlarged view of the same plot.

The constraint on $f_{\rm PBH}$ is obtained by marginalizing over the mass function width σ and $\Omega_{\rm CBC}$.

For $M_{\rm PBH} \gtrsim 3\times10^2 M_\odot$, the GWB spectral amplitude is dominated by the late binary formation channel. Although the LVK loses its constraining power sharply in this mass range due to the limited frequency range, this suggests an interesting possibility for constraining this mass range using the late binary formation channel with the Einstein Telescope [102,103] and Cosmic Explorer [104,105], which have greater sensitivity at low frequencies. We also demonstrate that Advanced LIGO A+ can provide valuable information about the underlying background. See Appendix C for one such scenario.

These findings demonstrate that GWB constraints are and will continue to be a vital probe, particularly within the mass range $[10^1, 3\times10^2]M_\odot$. Our results improve the previous GWB constraints [27,40,51] by $O(2\sim10)$ at $100M_\odot$ with the latest publicly available LVK observing run data.

TABLE II. 95% CL on $f_{\rm PBH}$ at various masses.

	μ		
$R_{\rm clust}$	$1[M_\odot]$	$30[M_\odot]$	$10^3[M_\odot]$
1	3.6×10^{-2}	5.3×10^{-3}	1.0×10^{0}
4×10^2	4.0×10^{-2}	6.2×10^{-3}	5.8×10^{-1}
10^3	3.3×10^{-2}	5.8×10^{-3}	4.8×10^{-1}

IV. CONCLUSION

In this study, we conducted a targeted search for a GWB originating from PBHs using cross-correlation data from the first three observing runs of the LVK collaboration [56–58]. Unlike previous research that focused on the population of resolved GW events, we utilized cross-correlated LVK data specifically to search for a GWB resulting from the superposition of many unresolved binary events. Our mass range encompasses PBH binaries with component masses both below and above those detected in the LVK catalog [2,4].

Our approach advances beyond previous stochastic analyses that utilized the LVK upper limit derived under the assumption of a power-law shape for the spectrum. By directly modeling the expected GWB signal from PBH mergers, we present, for the first time, a direct GWB search specifically targeting PBH mergers.

Although we did not find significant evidence for a GWB from PBHs, we established new constraints on the fraction of PBHs contributing to the current dark matter energy density, $f_{\rm PBH}$, as a function of PBH mass assuming a log-normal mass distribution. These constraints complement existing bounds from individual CBC events [25,27,34] and other observational methods such as microlensing and cosmic microwave background observations [97–100].

Future constraints will undoubtedly provide deeper and broader insights into the abundance of PBHs across a wider mass range and will offer valuable information for pinpointing the origin of black holes. Additionally, the broad mass function, in particular those predicted by QCD phase transitions, remains an interesting case for investigation. In future work, we plan to apply our analysis to this model

using more accurate descriptions of their merger rates that are currently under development.

The software packages used were Matplotlib [106], NumPy [107], SciPy [108], Dynesty [95], PYGWB [81], and PBHBounds [101].

ACKNOWLEDGMENTS

The authors would like to thank Vuk Mandic and the LVK Stochastic group for comments. This research has made use of data or software obtained from the Gravitational Wave Open Science Center [109], a service of the LIGO Scientific Collaboration, the Virgo Collaboration, and KAGRA. This material is based upon work supported by LIGO Laboratory which is a major facility fully funded by the National Science Foundation, as well as the Science and Technology Facilities Council (STFC) of the United Kingdom, the Max-Planck-Society (MPS), and the State of Niedersachsen/Germany for support of the construction of Advanced LIGO and construction and operation of the GEO600 detector. Additional support for Advanced LIGO was provided by the Australian Research Council. Virgo is funded, through the European Gravitational Observatory (EGO), by the French Centre National de Recherche Scientifique (CNRS), the Italian Istituto Nazionale di Fisica Nucleare (INFN), and the Dutch Nikhef, with contributions by institutions from Belgium, Germany, Greece, Hungary, Ireland, Japan, Monaco, Poland, Portugal, and Spain. KAGRA is supported by Ministry of Education, Culture, Sports, Science and Technology (MEXT), Japan Society for the Promotion of Science (JSPS) in Japan; National Research Foundation (NRF) and Ministry of Science and ICT (MSIT) in Korea; Academia Sinica (AS) and National Science and Technology Council (NSTC) in Taiwan. S. C. acknowledges support from the Belgian Fund for Research FNRS-FRS through an Incentive Grant For Scientific Research and through the IISN convention 4.4501.19. S. K. is supported by the Spanish Attraccion de Talento Contract No. 2023-5A-TIC-28945 granted by the Comunidad de Madrid, the I + D Grant No. PID2023-149018NB-C42, and the Grant IFT Centro de Excelencia Severo Ochoa No. CEX2020-001007-S funded by MCIN/AEI/10.13039/501100011033, the Consolidación Investigadora 2022 Grant No. CNS2022-135211, and Japan Society for the Promotion of Science (JSPS) KAKENHI Grants No. JP20H05853, No. JP23H00110, and No. JP24K00624. M. S. acknowledges support from the Science and Technology Facility Council (STFC), UK, under the Research Grant No. ST/X000753/1.

This manuscript was assigned LIGO-Document No. LIGO-P2400579.

DATA AVAILABILITY

The data that support the findings of this article are openly available [109].

APPENDIX A: MODELS FOR SUPPRESSION FACTORS

Here we give for completeness the models for binary suppression factors for early PBH binaries that are studied in [26,27].

The suppression factor is expressed as the product of S_1 and S_2. The first factor, S_1, describes the disruption of binaries due to either matter fluctuations or the influence of a nearby PBH. It is given by

$$S_1 \approx 1.42 \left[\frac{(\langle m_{\rm PBH}^2 \rangle / \langle m_{\rm PBH} \rangle^2)}{\bar{N} + C} + \frac{\sigma_{\rm M}^2}{f_{\rm PBH}^2} \right]^{-21/74} {\rm e}^{-\bar{N}}, \tag{A1}$$

where $\sigma_{\bar{M}} = 0.005$ is the variance of matter density perturbations, evaluated at binary formation, and $\bar{N}$ is the number of PBHs within a sphere of comoving radius around the initial PBH pair, given by

$$\bar{N} = \frac{m_1 + m_2}{\langle m_{\rm PBH} \rangle} \frac{f_{\rm PBH}}{f_{\rm PBH} + \sigma_M}. \tag{A2}$$

In Eqs. (A1) and (A2), the mean PBH mass and their variance are calculated from the mass function through

$$\begin{aligned} \langle m_{\rm PBH} \rangle &= \frac{\int m_{\rm PBH} {\rm d}n_{\rm PBH}}{n_{\rm PBH}} \\ &= \left[\int \frac{f(m_{\rm PBH})}{m_{\rm PBH}} {\rm d}\ \ln\ m_{\rm PBH} \right]^{-1} \end{aligned} \tag{A3}$$

$$\begin{aligned} \langle m_{\rm PBH}^2 \rangle &= \frac{\int m_{\rm PBH}^2 {\rm d}n_{\rm PBH}}{n_{\rm PBH}} \\ &= \frac{\int m_{\rm PBH} f(m_{\rm PBH}) {\rm d}\ \ln\ m_{\rm PBH}}{\int \frac{f(m_{\rm PBH})}{m_{\rm PBH}} {\rm d}\ \ln\ m_{\rm PBH}}, \end{aligned} \tag{A4}$$

where $n_{\rm PBH}$ denotes the total PBH number density. The function C encodes the transition between small and large $\bar{N}$ limits. A good approximation is

$$\begin{aligned} C \simeq & \frac{f_{\rm PBH}^2 \langle m_{\rm PBH}^2 \rangle}{\sigma_{\rm M}^2 \langle m_{\rm PBH} \rangle^2} \\ & \times \left\{ \left[\frac{\Gamma(29/37)}{\sqrt{\pi}} U\left(\frac{21}{74}, \frac{1}{2}, \frac{5 f_{\rm PBH}^2}{6\sigma_{\rm M}^2} \right) \right]^{-74/21} - 1 \right\}^{-1}, \end{aligned} \tag{A5}$$

where Γ is the Euler function and U is the confluent hypergeometric function.

The second factor, S_2, captures the impact of binary disruption within PBH clusters that can form rapidly following PBH formation, provided their abundance is sufficiently high, as a result of initial Poisson fluctuations.

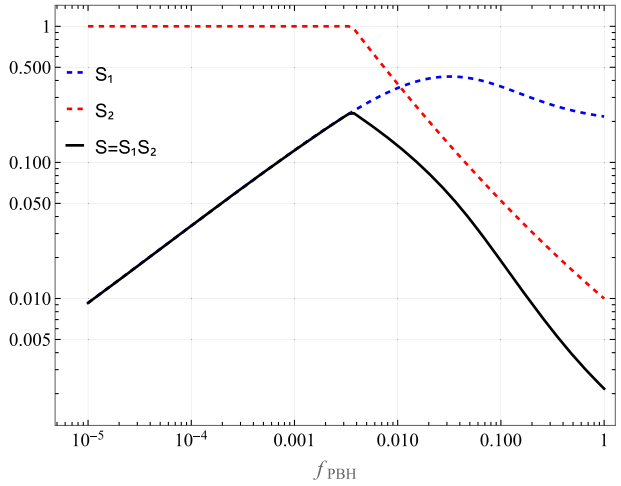


FIG. 2. Binary suppression factors for early binary formation are presented as a function of $f_{\rm PBH}$ for a narrow mass distribution. See also Fig. 20 in [110].

It can be approximated by

$$S_2 \approx \min\left(1, 9.6\times 10^{-3} f_{\rm PBH}^{-0.65} e^{0.03\ln^2 f_{\rm PBH}}\right). \quad \text{(A6)}$$

We plot S_1 and S_2 in Fig. 2 as a function of $f_{\rm PBH}$ for a narrow mass distribution, in which case the above functions have simpler forms, since we can approximate $\langle m_{\rm PBH}^2\rangle/\langle m_{\rm PBH}\rangle^2 \approx 1$ and $m_1 + m_2/\langle m_{\rm PBH}\rangle \approx 2$. Note that the validity of the above expressions for a broad mass distribution necessitates detailed analytical investigation or validation through N-body simulations. When considering a wide range of masses, the system exhibits a richer phenomenology, including, for example, the presence of PBHs that stimulate cluster formation, as well as smaller PBHs that could dominate the calculation of $\bar{N}$ without being sufficiently massive to disrupt a significant binary system (we refer the reader to Sec. 4.1.6 of [110] for more details). Furthermore, it is important to recognize that early binaries can be significantly affected by their environment throughout cosmic history. This environment undergoes complex evolution driven by factors such as cluster formation following matter-radiation equality, accretion processes, and dynamical heating. As a result, one should exercise caution, as making claims based on these merging rates may be premature. This aspect will be further emphasized in scenarios where PBHs exhibit a broad mass distribution. PBH clusters with varying mass black holes would display a complex array of phenomena, including mass segregation and the ejection of smaller black holes due to kicks, etc. Currently, we have not yet achieved a comprehensive understanding of such scenarios; therefore, in this study, we concentrate on the case of a narrow mass distribution.

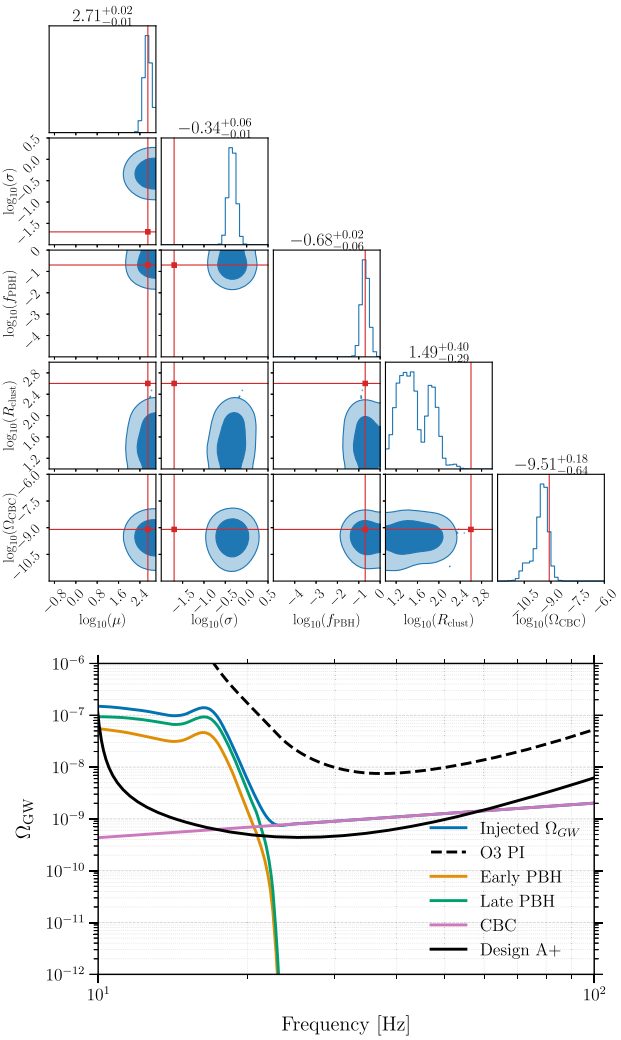


FIG. 3. Top: posterior distributions from the injection study with true values. The diagonal panels show the 1D marginals with the injected values marked by red lines, and the off-diagonal panels show the 2D joint posteriors with 68% and 95% credible contours. Bottom: components of the signal with sensitivity curves.

APPENDIX B: CROSS-CORRELATION STATISTICS

To estimate the GWB, the strain data from each GW detector, denoted by $s_i(t)$, are divided into segments of duration T. This segmentation helps mitigate the effects of nonstationarities and data interruptions. For each segment t_i and for every pair of detectors I and J (referred to as a baseline), the cross spectral density $\hat{C}_{IJ,t_i}(f_j)$ is calculated at discrete frequency bins f_j. The cross spectral density is given by

$$\hat{C}^{IJ}_{t_i,f_j} = \frac{2}{T}\mathrm{Re}\left[s^{*I}_{t_i,f_j} s^{J}_{t_i,f_j}\right], \quad \text{(B1)}$$

where $s^{I}_{t_i,f_j}$ represents the Fourier transform of the time series from detector I within segment t_i at frequency f_j.

Next, the optimal cross-correlation statistic for GWB, $\hat{\Omega}^{IJ}_{t_i,f_j}$ and its associated variance $\hat{\sigma}^{IJ}_{t_i,f_j}$ are constructed to maximize the signal-to-noise ratio (SNR) for each narrow frequency bin f_j. These are obtained as [81,111,112]

$$\hat{\Omega}^{IJ}_{t_i,f_j} = \frac{\hat{C}_{IJ,t_i}(f_j)}{\gamma_{IJ}(f_j)S_0(f_j)}, \tag{B2}$$

$$\left(\hat{\sigma}^{IJ}_{t_i,f_j}\right)^2 = \frac{1}{2T\Delta f}\cdot\frac{P_{1,t_i}(f_j)P_{2,t_i}(f_j)}{\gamma^2_{IJ}(f_j)S^2_0(f_j)}, \tag{B3}$$

where $\gamma_{IJ}(f_j)$ is the overlap reduction function for the baseline IJ, $S_0(f) = \frac{10\pi^2 f^3}{3H_0^2}$ is the normalization factor with H_0 being the Hubble constant, and $\Delta f = f_{j+1} - f_j$ is the width of the frequency bin centered at f_j. Additionally, $P_{1,t_i}(f_j)$ and $P_{2,t_i}(f_j)$ are the power spectral densities of detectors I and J in segment t_i at frequency f_j.

Then, different segments can be combined with weights $1/(\hat{\sigma}^{IJ}_{t_i,f_j})^2$ to obtain averaged GWB spectra,

$$\hat{\Omega}^{IJ}_{\mathrm{GW},f_j} = \frac{\sum_i \hat{\Omega}^{IJ}_{t_i,f_j}(\hat{\sigma}^{IJ}_{t_i,f_j})^{-2}}{\sum_i (\hat{\sigma}^{IJ}_{t_i,f_j})^{-2}}, \tag{B4}$$

which is being used in constructing the likelihood in Eq. (7).

APPENDIX C: INJECTION STUDY

In order to validate the Bayesian formalism described in the text and provide a possible interesting scenario, we performed an injection study by adding a synthetic GWB signal,

$$\Omega_{\mathrm{GW}}(f) = \Omega_{\mathrm{EB}}(f) + \Omega_{\mathrm{LB}}(f) + \Omega_{\mathrm{CBC}}(f).$$

We injected our model with the parameter values,

$$(\mu, \sigma, f_{\mathrm{PBH}}, R_{\mathrm{clust}}, \Omega_{\mathrm{CBC}}) = (5\times 10^2 M_\odot, 2\times 10^{-2}, 2\times 10^{-1}, 4\times 10^2, 8\times 10^{-10}),$$

to the projected Advanced LIGO A+ sensitivity curve. The injected spectrum was chosen such that it lies below the O3 power law integrated (PI) curve but above the A+ sensitivity. Recovery with our nested-sampling pipeline yielded accurate posterior constraints on the primary parameters μ, f_{PBH} as shown in Fig. 3 and Ω_{CBC}; however, R_{clust} and σ were not well recovered. This behavior arises because the spectral cutoff induced by σ has only a mild impact on the overall shape, making σ difficult to constrain, and because the late-binary component is subdominant, reducing sensitivity to R_{clust}. These findings are corroborated by the corner plots presented in Appendix D, which show an essentially flat posterior for σ, and by the upper-limit curves in the main text, which exhibit only a weak dependence on R_{clust}.

APPENDIX D: CORNER PLOTS

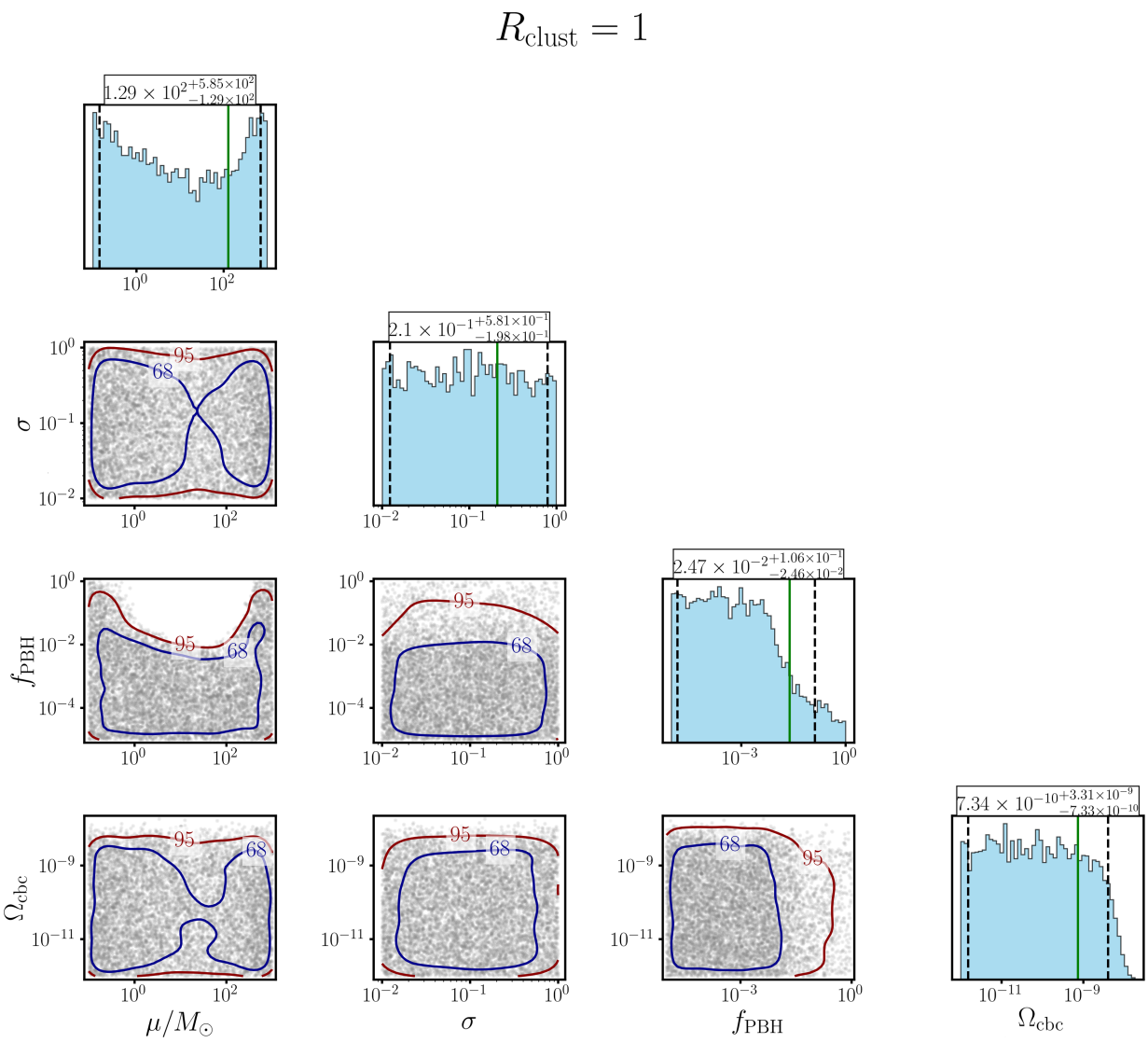


FIG. 4. Corner plots of posteriors for $R_{\rm clust} = 1$ used in the analysis.

$$R_{\rm clust} = 4 \times 10^2$$

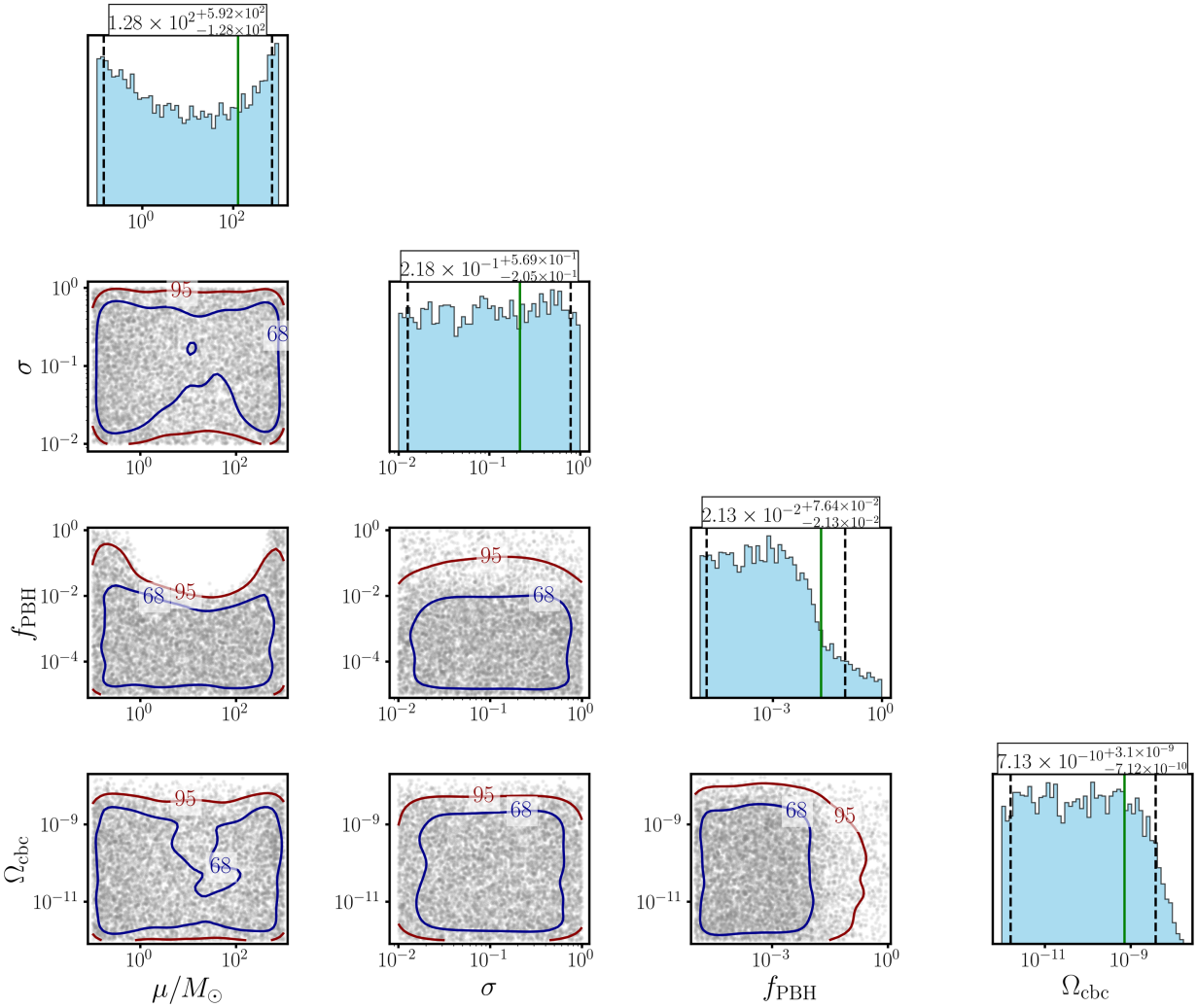


FIG. 5. Corner plots of posteriors for $R_{\rm clust} = 4 \times 10^2$ used in the analysis.

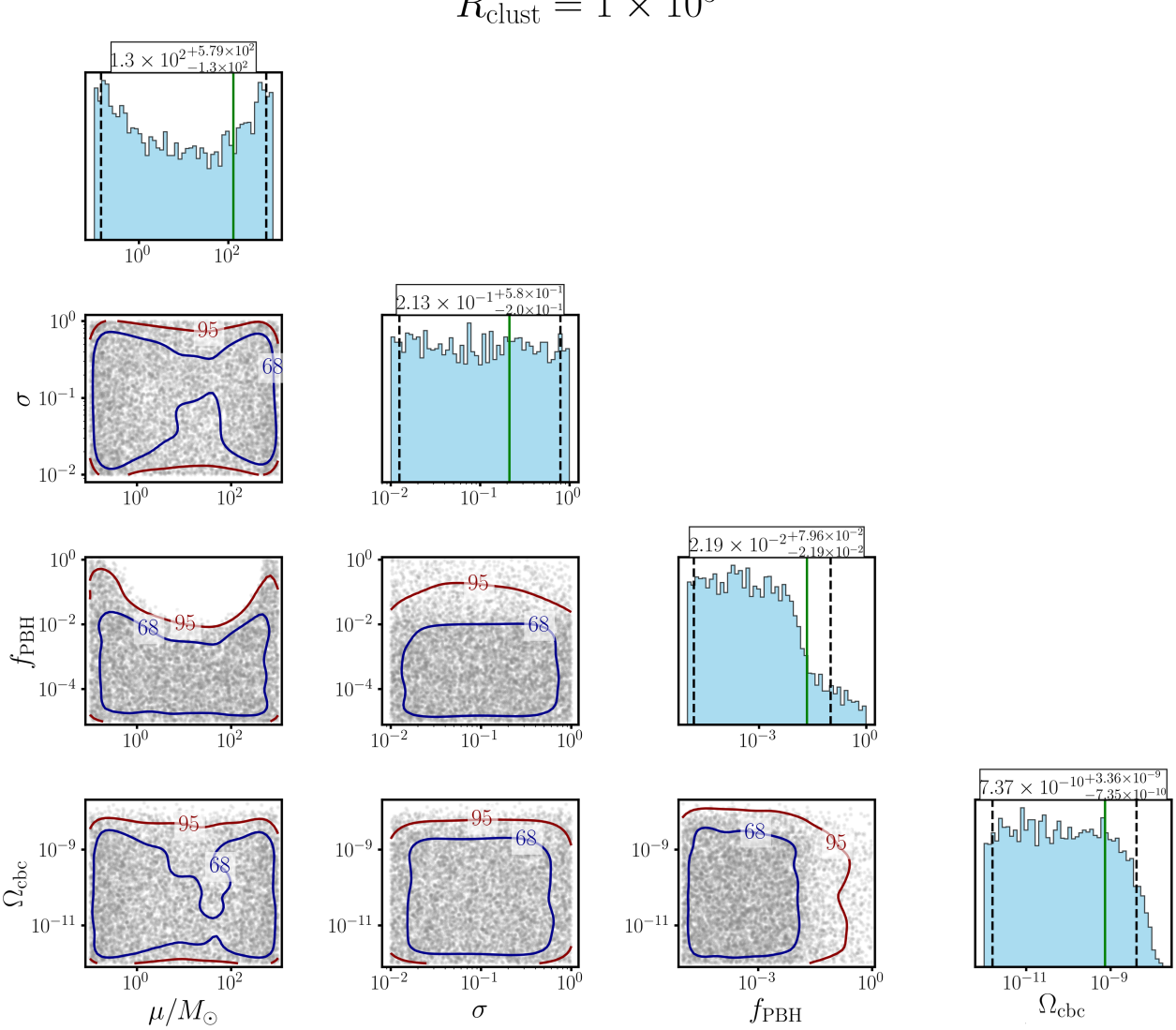


FIG. 6. Corner plots of posteriors for $R_{\rm clust} = 10^3$ used in the analysis.

[1] B. P. Abbott *et al.*, Observation of gravitational waves from a binary black hole merger, Phys. Rev. Lett. **116**, 061102 (2016).

[2] B. P. Abbott *et al.*, GWTC-1: A gravitational-wave transient catalog of compact binary mergers observed by LIGO and Virgo during the first and second observing runs, Phys. Rev. X **9**, 031040 (2019).

[3] Richard Abbott, T. D. Abbott, S. Abraham, F. Acernese, K. Ackley, A. Adams, C. Adams, R. X. Adhikari, V. B. Adya, Christoph Affeldt *et al.*, GWTC-2: Compact binary coalescences observed by LIGO and Virgo during the first half of the third observing run, Phys. Rev. X **11**, 021053 (2021).

[4] R. Abbott *et al.*, GWTC-3: Compact binary coalescences observed by LIGO and Virgo during the second part of the third observing run, Phys. Rev. X **13**, 041039 (2023).

[5] R. Abbott *et al.*, Tests of general relativity with binary black holes from the second LIGO-Virgo gravitational-wave transient catalog, Phys. Rev. D **103**, 122002 (2021).

[6] R. Abbott *et al.*, Constraints on the cosmic expansion history from GWTC–3, Astrophys. J. **949**, 76 (2023).

[7] Tania Regimbau, The astrophysical gravitational wave stochastic background, Res. Astron. Astrophys. **11**, 369 (2011).

[8] Arthur Kosowsky, Michael S. Turner, and Richard Watkins, Gravitational radiation from colliding vacuum bubbles, Phys. Rev. D **45**, 4514 (1992).

[9] Alba Romero, Katarina Martinovic, Thomas A. Callister, Huai-Ke Guo, Mario Martínez, Mairi Sakellariadou, Feng-Wei Yang, and Yue Zhao, Implications for first-order cosmological phase transitions from the third LIGO-Virgo observing run, Phys. Rev. Lett. **126**, 151301 (2021).

[10] Thibault Damour and Alexander Vilenkin, Gravitational wave bursts from cosmic strings, Phys. Rev. Lett. **85**, 3761 (2000).

[11] R. Abbott *et al.*, Constraints on cosmic strings using data from the third Advanced LIGO–Virgo observing run, Phys. Rev. Lett. **126**, 241102 (2021).

[12] Alexei A. Starobinsky, Spectrum of relict gravitational radiation and the early state of the universe, JETP Lett. **30**, 682 (1979), https://ui.adsabs.harvard.edu/abs/1979ZhPmR..30..719S/abstract.

[13] Chiara Caprini and Daniel G. Figueroa, Cosmological backgrounds of gravitational waves, Classical Quantum Gravity **35**, 163001 (2018).

[14] Mairi Sakellariadou, Gravitational waves: The theorist's swiss knife, Universe **8**, 132 (2022).

[15] Stephen Hawking, Gravitationally collapsed objects of very low mass, Mon. Not. R. Astron. Soc. **152**, 75 (1971).

[16] George F Chapline, Cosmological effects of primordial black holes, Nature (London) **253**, 251 (1975).

[17] Bernard Carr and Florian Kuhnel, Primordial black holes as dark matter candidates, SciPost Phys. Lect. Notes **48**, 1 (2022).

[18] Anne M. Green and Bradley J. Kavanagh, Primordial black holes as a dark matter candidate, J. Phys. G **48**, 043001 (2021).

[19] Simeon Bird, Ilias Cholis, Julian B. Muñoz, Yacine Ali-Haïmoud, Marc Kamionkowski, Ely D. Kovetz, Alvise Raccanelli, and Adam G. Riess, Did LIGO detect dark matter?, Phys. Rev. Lett. **116**, 201301 (2016).

[20] Misao Sasaki, Teruaki Suyama, Takahiro Tanaka, and Shuichiro Yokoyama, Primordial black hole scenario for the gravitational-wave event GW150914, Phys. Rev. Lett. **117**, 061101 (2016); **121**, 059901(E) (2018).

[21] Sebastien Clesse and Juan García-Bellido, The clustering of massive primordial black holes as dark matter: Measuring their mass distribution with Advanced LIGO, Phys. Dark Universe **15**, 142 (2017).

[22] Richard Abbott, T. D. Abbott, S. Abraham, F. Acernese, K. Ackley, C. Adams, R. X. Adhikari, V. B. Adya, C. Affeldt, M. Agathos *et al.*, Properties and astrophysical implications of the 150 $M_\odot$ binary black hole merger GW190521, Astrophys. J. Lett. **900**, L13 (2020).

[23] Yacine Ali-Haïmoud, Ely D. Kovetz, and Marc Kamionkowski, Merger rate of primordial black-hole binaries, Phys. Rev. D **96**, 123523 (2017).

[24] Sebastien Clesse and Juan García-Bellido, Seven hints for primordial black hole dark matter, Phys. Dark Universe **22**, 137 (2018).

[25] Martti Raidal, Ville Vaskonen, and Hardi Veermäe, Gravitational waves from primordial black hole mergers, J. Cosmol. Astropart. Phys. 09 (2017) 037.

[26] Martti Raidal, Christian Spethmann, Ville Vaskonen, and Hardi Veermäe, Formation and evolution of primordial black hole binaries in the early universe, J. Cosmol. Astropart. Phys. 02 (2019) 018.

[27] Gert Hütsi, Martti Raidal, Ville Vaskonen, and Hardi Veermäe, Two populations of LIGO-Virgo black holes, J. Cosmol. Astropart. Phys. 03 (2021) 068.

[28] Ville Vaskonen and Hardi Veermäe, Lower bound on the primordial black hole merger rate, Phys. Rev. D **101**, 043015 (2020).

[29] Zu-Cheng Chen, Chen Yuan, and Qing-Guo Huang, Pulsar timing array constraints on primordial black holes with NANOGrav 11-year dataset, Phys. Rev. Lett. **124**, 251101 (2020).

[30] Sebastien Clesse and Juan Garcia-Bellido, GW190425, GW190521 and GW190814: Three candidate mergers of primordial black holes from the QCD epoch, Phys. Dark Universe **38**, 101111 (2022).

[31] V. De Luca, V. Desjacques, G. Franciolini, P. Pani, and A. Riotto, GW190521 mass gap event and the primordial black hole scenario, Phys. Rev. Lett. **126**, 051101 (2021).

[32] Kenta Ando, Keisuke Inomata, and Masahiro Kawasaki, Primordial black holes and uncertainties in the choice of the window function, Phys. Rev. D **97**, 103528 (2018).

[33] S. Blinnikov, A. Dolgov, N. K. Porayko, and K. Postnov, Solving puzzles of GW150914 by primordial black holes, J. Cosmol. Astropart. Phys. 11 (2016) 036.

[34] Alex Hall, Andrew D. Gow, and Christian T. Byrnes, Bayesian analysis of LIGO-Virgo mergers: Primordial vs, astrophysical black hole populations, Phys. Rev. D **102**, 123524 (2020).

[35] Kaze W. K. Wong, Gabriele Franciolini, Valerio De Luca, Vishal Baibhav, Emanuele Berti, Paolo Pani, and Antonio Riotto, Constraining the primordial black hole scenario with Bayesian inference and machine learning: The GWTC-2 gravitational wave catalog, Phys. Rev. D **103**, 023026 (2021).

[36] Karsten Jedamzik, Consistency of primordial black hole dark matter with LIGO/Virgo merger rates, Phys. Rev. Lett. **126**, 051302 (2021).

[37] V. De Luca, G. Franciolini, P. Pani, and A. Riotto, Bayesian evidence for both astrophysical and primordial black holes: Mapping the GWTC-2 catalog to third-generation detectors, J. Cosmol. Astropart. Phys. 05 (2021) 003.

[38] Bin Liu and Dong Lai, Hierarchical black-hole mergers in multiple systems: Constrain the formation of GW190412, GW190814 and GW190521-like events, Mon. Not. R. Astron. Soc. **502**, 2049 (2021).

[39] Kyriakos Vattis, Isabelle S. Goldstein, and Savvas M. Koushiappas, Could the 2.6$M_\odot$ object in GW190814 be a primordial black hole?, Phys. Rev. D **102**, 061301 (2020).

[40] V. De Luca, G. Franciolini, P. Pani, and A. Riotto, Primordial black holes confront LIGO/Virgo data: Current situation, J. Cosmol. Astropart. Phys. 06 (2020) 044.

[41] Zu-Cheng Chen and Alex Hall, *Confronting Primordial Black Holes with LIGO-Virgo-KAGRA and the Einstein Telescope* (Springer Nature, Singapore, 2025), pp. 617–650.

[42] Suvodip Mukherjee and Joseph Silk, Can we distinguish astrophysical from primordial black holes via the stochastic gravitational wave background?, Mon. Not. R. Astron. Soc. **506**, 3977 (2021).

[43] Richard Abbott, T. D. Abbott, S. Abraham, Fausto Acernese, K. Ackley, C. Adams, R. X. Adhikari, V. B. Adya, Christoph Affeldt, M. Agathos *et al.*, GW190521: A binary black hole merger with a total mass of $150\,M_{\odot}$, Phys. Rev. Lett. **125**, 101102 (2020).

[44] Gabriele Franciolini, Vishal Baibhav, Valerio De Luca, Ken K. Y. Ng, Kaze W. K. Wong, Emanuele Berti, Paolo Pani, Antonio Riotto, and Salvatore Vitale, Searching for a subpopulation of primordial black holes in LIGO-Virgo gravitational-wave data, Phys. Rev. D **105**, 083526 (2022).

[45] Alexander H. Nitz and Yi-Fan Wang, Broad search for gravitational waves from subsolar-mass binaries through LIGO and Virgo's third observing run, Phys. Rev. D **106**, 023024 (2022).

[46] Khun Sang Phukon, Gregory Baltus, Sarah Caudill, Sebastien Clesse, Antoine Depasse, Maxime Fays, Heather Fong, Shasvath J. Kapadia, Ryan Magee, and Andres Jorge Tanasijczuk, The Hunt for sub-solar primordial black holes in low mass ratio binaries is open, arXiv:2105.11449.

[47] LVK collaboration, Search for subsolar-mass black hole binaries in the second part of Advanced LIGO's and Advanced Virgo's third observing run, Mon. Not. R. Astron. Soc. **524**, 5984 (2023); **526**, 6234(E) (2023).

[48] Andrew L. Miller, Nancy Aggarwal, Sébastien Clesse, Federico De Lillo, Surabhi Sachdev, Pia Astone, Cristiano Palomba, Ornella J. Piccinni, and Lorenzo Pierini, Gravitational wave constraints on planetary-mass primordial black holes using LIGO O3a data, Phys. Rev. Lett. **133**, 111401 (2024).

[49] Céline Boehm, Archil Kobakhidze, Ciaran A. J. O'hare, Zachary S. C. Picker, and Mairi Sakellariadou, Eliminating the LIGO bounds on primordial black hole dark matter, J. Cosmol. Astropart. Phys. 03 (2021) 078.

[50] Vuk Mandic, Simeon Bird, and Ilias Cholis, Stochastic gravitational-wave background due to primordial binary black hole mergers, Phys. Rev. Lett. **117**, 201102 (2016).

[51] Sai Wang, Yi-Fan Wang, Qing-Guo Huang, and Tjonnie GF Li, Constraints on the primordial black hole abundance from the first Advanced LIGO observation run using the stochastic gravitational-wave background, Phys. Rev. Lett. **120**, 191102 (2018).

[52] Keisuke Inomata, Kazunori Kohri, and Takahiro Terada, Detected stochastic gravitational waves and subsolar-mass primordial black holes, Phys. Rev. D **109**, 063506 (2024).

[53] Suvodip Mukherjee, Matthew S. P. Meinema, and Joseph Silk, Prospects of discovering subsolar primordial black holes using the stochastic gravitational wave background from third-generation detectors, Mon. Not. R. Astron. Soc. **510**, 6218 (2022).

[54] Alba Romero-Rodríguez and Sachiko Kuroyanagi, *LIGO-Virgo-KAGRA Constraints on Primordial Black Holes from Stochastic Gravitational-Wave Background Searches* (Springer Nature, Singapore, 2025), pp. 651–688.

[55] Vicente Atal, Jose J. Blanco-Pillado, Albert Sanglas, and Nikolaos Triantafyllou, Constraining changes in the merger history of BH and PBH binaries with the stochastic gravitational wave background, Phys. Rev. D **105**, 123522 (2022).

[56] Benjamin P. Abbott, Robert Abbott, Thomas D. Abbott, Matthew R. Abernathy, Fausto Acernese, Kendall Ackley, Carl Adams, Thomas Adams, Paolo Addesso, Rana X. Adhikari *et al.*, Upper limits on the stochastic gravitational-wave background from Advanced LIGO's first observing run, Phys. Rev. Lett. **118**, 121101 (2017).

[57] Benjamin P. Abbott, R. Abbott, T. D. Abbott, S. Abraham, F. Acernese, K. Ackley, C. Adams, V. B. Adya, C. Affeldt, M. Agathos *et al.*, Search for the isotropic stochastic background using data from Advanced LIGO's second observing run, Phys. Rev. D **100**, 061101 (2019).

[58] Ryan Abbott, T. D. Abbott, S. Abraham, Fausto Acernese, K. Ackley, A. Adams, C. Adams, Rana X. Adhikari, V. B. Adya, C. Affeldt *et al.*, Upper limits on the isotropic gravitational-wave background from Advanced LIGO and Advanced Virgo's third observing run, Phys. Rev. D **104**, 022004 (2021).

[59] Karsten Jedamzik, Primordial black hole formation during the QCD epoch, Phys. Rev. D **55**, R5871 (1997).

[60] Bernard Carr, Sebastien Clesse, Juan García-Bellido, and Florian Kühnel, Cosmic conundra explained by thermal history and primordial black holes, Phys. Dark Universe **31**, 100755 (2021).

[61] Bernard Carr, Sebastien Clesse, and Juan García-Bellido, Primordial black holes from the QCD epoch: Linking dark matter, baryogenesis and anthropic selection, Mon. Not. R. Astron. Soc. **501**, 1426 (2021).

[62] Andrew D. Gow, Christian T. Byrnes, and Alex Hall, Accurate model for the primordial black hole mass distribution from a peak in the power spectrum, Phys. Rev. D **105**, 023503 (2022).

[63] Alexandre Dolgov and Joseph Silk, Baryon isocurvature fluctuations at small scales and baryonic dark matter, Phys. Rev. D **47**, 4244 (1993).

[64] V. De Luca, G. Franciolini, and A. Riotto, On the primordial black hole mass function for broad spectra, Phys. Lett. B **807**, 135550 (2020).

[65] Giacomo Ferrante, Gabriele Franciolini, Antonio Iovino, Jr., and Alfredo Urbano, Primordial non-Gaussianity up to all orders: Theoretical aspects and implications for primordial black hole models, Phys. Rev. D **107**, 043520 (2023).

[66] Andrew D. Gow, Hooshyar Assadullahi, Joseph H. P. Jackson, Kazuya Koyama, Vincent Vennin, and David Wands, Non-perturbative non-Gaussianity and primordial black holes, Europhys. Lett. **142**, 49001 (2023).

[67] E. S. Phinney, A practical theorem on gravitational wave backgrounds, arXiv:astro-ph/0108028.

[68] P. Ajith, Mark Hannam, Sascha Husa, Yanbei Chen, B. Brügmann, Nils Dorband, D. Müller, Frank Ohme, Denis Pollney, Christian Reisswig *et al.*, Inspiral-merger-ringdown waveforms for black-hole binaries with non-precessing spins, Phys. Rev. Lett. **106**, 241101 (2011).

[69] Takashi Nakamura, Misao Sasaki, Takahiro Tanaka, and Kip S. Thorne, Gravitational waves from coalescing black hole MACHO binaries, Astrophys. J. Lett. **487**, L139 (1997).

[70] Kunihito Ioka, Takeshi Chiba, Takahiro Tanaka, and Takashi Nakamura, Black hole binary formation in the expanding universe: Three body problem approximation, Phys. Rev. D **58**, 063003 (1998).

[71] Bence Kocsis, Teruaki Suyama, Takahiro Tanaka, and Shuichiro Yokoyama, Hidden universality in the merger rate distribution in the primordial black hole scenario, Astrophys. J. **854**, 41 (2018).

[72] Gerald D. Quinlan and Stuart L. Shapiro, Dynamical evolution of dense clusters of compact stars, Astrophys. J. **343**, 725 (1989).

[73] Hideaki Mouri and Yoshiaki Taniguchi, Runaway merging of black holes: Analytical constraint on the timescale, Astrophys. J. Lett. **566**, L17 (2002).

[74] Simeon Bird, Ilias Cholis, Julian B. Muñoz, Yacine Ali-Haïmoud, Marc Kamionkowski, Ely D. Kovetz, Alvise Raccanelli, and Adam G. Riess, Did LIGO detect dark matter?, Phys. Rev. Lett. **116**, 201301 (2016).

[75] Eleni Bagui and Sebastien Clesse, A boosted gravitational wave background for primordial black holes with broad mass distributions and thermal features, Phys. Dark Universe **38**, 101115 (2022).

[76] Vuk Mandic, Eric Thrane, Stefanos Giampanis, and Tania Regimbau, Parameter estimation in searches for the stochastic gravitational-wave background, Phys. Rev. Lett. **109**, 171102 (2012).

[77] Katarina Martinovic, Charles Badger, Mairi Sakellariadou, and Vuk Mandic, Searching for parity violation with the LIGO-Virgo-KAGRA network, Phys. Rev. D **104**, L081101 (2021).

[78] Alba Romero-Rodriguez, Mario Martinez, Oriol Pujolas, Mairi Sakellariadou, and Ville Vaskonen, Search for a scalar induced stochastic gravitational wave background in the third LIGO-Virgo observing run, Phys. Rev. Lett. **128**, 051301 (2022).

[79] Charles Badger, Bartosz Fornal, Katarina Martinovic, Alba Romero, Kevin Turbang, Huai-Ke Guo, Alberto Mariotti, Mairi Sakellariadou, Alexander Sevrin, Feng-Wei Yang *et al.*, Probing early universe supercooled phase transitions with gravitational wave data, Phys. Rev. D **107**, 023511 (2023).

[80] Charles Badger, Hannah Duval, Tomohiro Fujita, Sachiko Kuroyanagi, Alba Romero-Rodríguez, and Mairi Sakellariadou, Detection prospects of gravitational waves from su(2) axion inflation, Phys. Rev. D **110**, 084063 (2024).

[81] Arianna I Renzini, Alba Romero-Rodríguez, Colm Talbot, Max Lalleman, Shivaraj Kandhasamy, Kevin Turbang, Sylvia Biscoveanu, Katarina Martinovic, Patrick Meyers, Leo Tsukada *et al.*, PYGWB: A Python-based library for gravitational-wave background searches, Astrophys. J. **952**, 25 (2023).

[82] Cheng-Jian Wu, Vuk Mandic, and Tania Regimbau, Accessibility of the stochastic gravitational wave background from magnetars to the interferometric gravitational wave detectors, Phys. Rev. D **87**, 042002 (2013).

[83] S. G. Crowder, R. Namba, V. Mandic, S. Mukohyama, and M. Peloso, Measurement of parity violation in the early universe using gravitational-wave detectors, Phys. Lett. B **726**, 66 (2013).

[84] Kyle Crocker, V. Mandic, T. Regimbau, K. Belczynski, W. Gladysz, K. Olive, T. Prestegard, and E. Vangioni, Model of the stochastic gravitational-wave background due to core collapse to black holes, Phys. Rev. D **92**, 063005 (2015).

[85] Margot Fitz Axen, Sharan Banagiri, Andrew Matas, Chiara Caprini, and Vuk Mandic, Multiwavelength observations of cosmological phase transitions using lisa and cosmic explorer, Phys. Rev. D **98**, 103508 (2018).

[86] Fausto Acernese, M. Agathos, L. Aiello, A. Allocca, A. Amato, S. Ansoldi, S. Antier, M. Arène, N. Arnaud, S. Ascenzi *et al.*, Increasing the astrophysical reach of the Advanced Virgo detector via the application of squeezed vacuum states of light, Phys. Rev. Lett. **123**, 231108 (2019).

[87] Benjamin P. Abbott, R. Abbott, T. D. Abbott, M. R. Abernathy, Fausto Acernese, K. Ackley, C. Adams, T. Adams, Paolo Addesso, R. X. Adhikari *et al.*, GW150914: The Advanced LIGO detectors in the era of first discoveries, Phys. Rev. Lett. **116**, 131103 (2016).

[88] Aaron Buikema, Craig Cahillane, G. L. Mansell, C. D. Blair, Robert Abbott, C. Adams, R. X. Adhikari, A. Ananyeva, S. Appert, K. Arai *et al.*, Sensitivity and performance of the Advanced LIGO detectors in the third observing run, Phys. Rev. D **102**, 062003 (2020).

[89] R. Abbott *et al.*, Open data from the third observing run of LIGO, Virgo, KAGRA, and GEO, Astrophys. J. Suppl. Ser. **267**, 29 (2023).

[90] John T. Whelan, Emma L. Robinson, Joseph D. Romano, and Eric H. Thrane, Treatment of calibration uncertainty in multi-baseline cross-correlation searches for gravitational waves, J. Phys. Conf. Ser. **484**, 012027 (2014).

[91] Ling Sun, Evan Goetz, Jeffrey S Kissel, Joseph Betzwieser, Sudarshan Karki, Aaron Viets, Madeline Wade, Dripta Bhattacharjee, Vladimir Bossilkov, Pep B. Covas *et al.*, Characterization of systematic error in Advanced LIGO calibration, Classical Quantum Gravity **37**, 225008 (2020).

[92] Thomas Callister, Letizia Sammut, Shi Qiu, Ilya Mandel, and Eric Thrane, Limits of astrophysics with gravitational-wave backgrounds, Phys. Rev. X **6**, 031018 (2016).

[93] Roberto Trotta, Bayes in the sky: Bayesian inference and model selection in cosmology, Contemp. Phys. **49**, 71 (2008).

[94] M. Andrés-Carcasona, A. J. Iovino, V. Vaskonen, H. Veermäe, M. Martínez, O. Pujolàs, and Ll. M. Mir, Constraints on primordial black holes from LIGO-Virgo-KAGRA O3 events, Phys. Rev. D **110**, 023040 (2024).

[95] Joshua S Speagle, Dynesty: A dynamic nested sampling package for estimating Bayesian posteriors and evidences, Mon. Not. R. Astron. Soc. **493**, 3132 (2020).

[96] Russel E. Caflisch, Monte Carlo and quasi-Monte Carlo methods, Acta Numer. **7**, 1 (1998).

[97] Patrick Tisserand, L. Le Guillou, C. Afonso, J. N. Albert, J. Andersen, R. Ansari, É Aubourg, P. Bareyre, J. P. Beaulieu, X. Charlot *et al.*, Limits on the macho content of the galactic halo from the EROS-2 survey of the magellanic clouds, Astron. Astrophys. **469**, 387 (2007).

[98] Przemek Mróz, Andrzej Udalski, Michał K. Szymański, Igor Soszyński, Łukasz Wyrzykowski, Paweł Pietrukowicz, Szymon Kozłowski, Radosław Poleski, Jan Skowron, Dorota Skowron *et al.*, No massive black holes in the Milky Way halo, Nature (London) **632**, 749 (2024).

[99] Miguel Zumalacarregui and Uroš Seljak, Limits on stellar-mass compact objects as dark matter from gravitational lensing of type IA supernovae, Phys. Rev. Lett. **121**, 141101 (2018).
[100] Dominic Agius, Rouven Essig, Daniele Gaggero, Francesca Scarcella, Gregory Suczewski, and Mauro Valli, Feedback in the dark: A critical examination of CMB bounds on primordial black holes, J. Cosmol. Astropart. Phys. 07 (2024) 003.
[101] Bradley J. Kavanagh, PBHBounds, https://github.com/bradkav/PBHbounds.
[102] M. Punturo *et al.*, The Einstein telescope: A third-generation gravitational wave observatory, Classical Quantum Gravity **27**, 194002 (2010).
[103] S. Hild, M. Abernathy, F. ea Acernese, P. Amaro-Seoane, N. Andersson, K. Arun, F. Barone, B. Barr, M. Barsuglia, M. Beker *et al.*, Sensitivity studies for third-generation gravitational wave observatories, Classical Quantum Gravity **28**, 094013 (2011).
[104] Benjamin P. Abbott, Richard Abbott, Thomas D. Abbott, Matthew R. Abernathy, Kendall Ackley, Carl Adams, Paolo Addesso, Rana X. Adhikari, Vaishali B. Adya, Christoph Affeldt *et al.*, Exploring the sensitivity of next generation gravitational wave detectors, Classical Quantum Gravity **34**, 044001 (2017).
[105] David Reitze *et al.*, Cosmic explorer: The U.S. contribution to gravitational-wave astronomy beyond LIGO, Bull. Am. Astron. Soc. **51**, 035 (2019), https://ui.adsabs.harvard.edu/abs/2019BAAS...51g..35R/abstract.
[106] John D. Hunter, Matplotlib: A 2d graphics environment, Comput. Sci. Eng. **9**, 90 (2007).
[107] Stefan Van Der Walt, S. Chris Colbert, and Gael Varoquaux, The NumPy array: A structure for efficient numerical computation, Comput. Sci. Eng. **13**, 22 (2011).
[108] Pauli Virtanen, Ralf Gommers, Travis E. Oliphant, Matt Haberland, Tyler Reddy, David Cournapeau, Evgeni Burovski, Pearu Peterson, Warren Weckesser, Jonathan Bright *et al.*, SciPy 1.0: Fundamental algorithms for scientific computing in Python, Nat. Methods **17**, 261 (2020).
[109] https://gwosc.org/
[110] Eleni Bagui *et al.*, Primordial black holes and their gravitational-wave signatures, Living Rev. Relativity **28**, 1 (2025).
[111] Bruce Allen and Joseph D. Romano, Detecting a stochastic background of gravitational radiation: Signal processing strategies and sensitivities, Phys. Rev. D **59**, 102001 (1999).
[112] Joseph D. Romano and Neil J. Cornish, Detection methods for stochastic gravitational-wave backgrounds: A unified treatment, Living Rev. Relativity **20**, 1 (2017).